Delay-Based Macromodels for Long Interconnects via Time-Frequency Decomposition

2006 IEEE Electrical Performance of Electronic Packaging

Delay-Based Macromodels for Long Interconnects via Time-Frequency Decompositions

S. Grivet-Talocia

Dip. Elettronica, Politecnico di Torino, C. Duca degli Abruzzi 24, 10129 Torino, Italy

Ph. +39 011 5644104, Fax +39 011 5644099 (e-mail grivet@polito.it)

Abstract: We introduce a new macromodeling scheme for electrically long interconnects characterized by tabulated frequency responses. The transfer function of the interconnect is modeled as a superposition of multiple single-delay atoms, which are identified via a selective inversion of a Gabor transform of the raw frequency data. Each atom is then approximated by a delayed rational function, leading to a highly-efficient SPICE-ready macromodel.

1 Introduction and motivations

Macromodeling techniques are now a standard tool for fast system-level simulation of interconnects. The interconnect structure of interest is first characterized via full-wave simulation or direct measurement in time or frequency domain, leading to the matrix transfer function of the structure. The latter is then processed by a suitable fitting algorithm in order to provide a closed-form approximation that can be synthesized into SPICE equivalent for system-level time-domain analysis.

Several macromodeling techniques are available according to different classes of structures. Interconnects that are electrically small at the highest frequency of interest can be approximated by lumped blocks characterized by rational transfer functions. Vector Fitting (VF) [1] is the standard tool for these structures. Long transmission lines can also be treated in this way since the propagation delay is known explicitly and can be extracted [2]. A complex interconnect link made of a chain of various blocks (Fig. 1) can be dealt with by first segmenting the structure into its basic parts, and then by macromodeling each part independently. Unfortunately, this procedure may lead to high-complexity global network which may take long simulation time for the computation of an eye diagram of the interconnect.

In this work, we explore another possibility based on a global low-complexity macromodel based on delayed rational approximations. We include multiple delay terms in the macromodel, which results then consistent with the electromagnetic behavior of the physical structure. Also, we suggest a procedure for the estimation of the macromodel parameters starting from external port characterization, including direct measurements.

We consider an arbitrary interconnect, as depicted in Fig. 1, made of a chain of cascaded blocks. Each of these blocks can be a transmission-line structure, a lumped block, or an electrically-long 3D interconnect (e.g., a connector, which cannot be described as a standard tramsmission line). The topology of the network can be even more complex than in Fig. 1, including ramifications, stubs, etc. The basic formulation applies to these more complex cases as well.

Let the interconnect structure be described by its scattering matrix $\boldsymbol{S}(s)$ defined at its external accessible ports. The internal ports are hidden in this description, but any discontinuity which is induced by the junctions of the various blocks has an effect. In time-domain, and with a suitable pulse excitation, this effect is visible as a reflected/transmitted distorted and attenuated echo of the excitation pulse, appearing at the external ports after a well-defined propagation delay. These considerations motivate the functional form which we assume for a global macromodel of the structure. Denoting as $\widehat{\boldsymbol{S}}(s)$ the scattering matrix of the model, we assume

$$\widehat{S}_{ij}(s) = \sum_k Q_{ij}^{(k)}(s) e^{-sT_k}, \quad Q_{ij}^{(k)} = \frac{N_{ij}^{(k)}(s)}{D_{ij}^{(k)}(s)}, \quad \text{with} \quad \widehat{S}_{ij}(j\omega) \simeq S_{ij}(j\omega) \tag{1}$$

over a prescribed frequency band, and where $N_{ij}^{(k)}(s)$, $D_{ij}^{(k)}(s)$ are polynomials of a suitable (small) order. It can be shown that the above formulation is exact when only ideal transmission lines and lumped blocks are present. If lossy lines and more complex structures are included, some approximation is obviously involved due to a finite number of echoes and to the rational approximation of the coefficients $Q_{ij}^{(k)}(s)$.

Similar representations have already been suggested in the macromodeling literature. The approach in [3] extracts only one dominant delay term and disregards higher order echoes. However, these can be quite important in the overall approximation, as we will demonstrate on practical examples. Also, this technique may fail when more the one delay is present in the raw data. Another approach (see [4] and references therein) and denoted as HPPM (Hybrid Phase-Pole Model) is a particular case of (1). In this work, only simple structures are considered, the delays are assumed

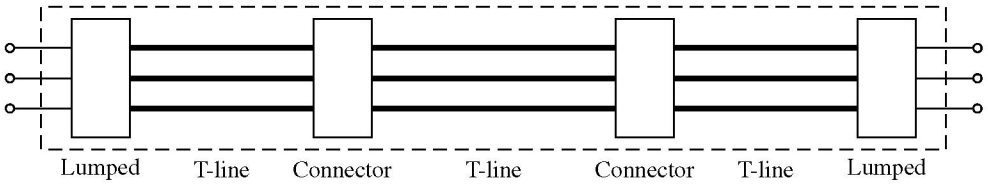

Figure 1: Interconnect structures under investigation, including an arbitrary number of transmission-line segments, lumped discontinuities, and more complex 3D interconnect blocks such as connectors.

to be analytically known, and the estimation of poles/residues of the approximation requires some prior time-domain simulation of the structure. Here, we rely only on tabulated frequency-domain samples at the external ports, and we provide a sound numerical procedure for the estimation of all macromodel parameters.

We will denote the elements $Q_{ij}^{(k)}(s)e^{-sT_k}$ in (1) as single-delay atoms. Our proposed method first provides a decomposition of $S_{ij}(s)$ into single-delay atoms based on an adaptive inversion of the so-called Gabor transform of the raw data. This is the subject of Sec. 2. Then, each atom is processed by extracting the (unique) delay and computing the rational approximation via standard techniques. Details are provided in Sec. 3. The numerical results of Sec. 4 illustrate the feasibility of the proposed approach for real interconnect structures. No details on SPICE implementation will be provided here since it requires standard methods.

2 Time-Frequency decomposition

The mathematical formulation is performed here on a generic scalar transfer function $H(\omega)$. We define the *Gabor* transform [6] of H as

$$\mathcal{G}(\omega,\tau)=\int_{-\infty}^{+\infty}H(\xi)W_{\omega,\tau}^{*}(\xi)d\xi\,,\quad W_{\omega,\tau}(\xi)=W(\xi-\omega)e^{-j\xi\tau}\,,\quad W(\xi)=\pi^{-1/4}e^{-\xi^{2}/2}\,. \tag{2}$$

The auxiliary function $W(\xi)$, namely a Gaussian with a normalization such that $||W||_2 = 1$, serves as a template to define the set of "basis" functions $W_{\omega,\tau}(\xi)$. These are defined in (2) as an amplitude-modulated (parameter τ is proportional to the number of oscillations) and translated (parameter ω is the center of the translation) version of $W(\xi)$. If $W(\xi)$ were taken to be identically one, the definition in (2) would become (up to a normalization constant) exactly the inverse Fourier transform of $H(\xi)$, which is the system impulse response $h(\tau)$. Hence, the variable τ has the physical meaning of time or time-delay. The Gaussian window $W(\xi)$ in (2) plays the role of a sharp bandpass filter. Therefore, $\mathcal{G}(\omega,\tau)$ can be regarded as the inverse Fourier transform of $H(\xi)$, but retaining only those frequency components located in a frequency band centered around ω. For this reson, $\mathcal{G}(\omega,\tau)$ belongs to the class of the so-called time-frequency transforms, since it provides a localization of the various components of H both in frequency ω and time τ.

The transform $\mathcal{G}(\omega,\tau)$ is highly redundant, since it is obtained by mapping a function of one variable $H(\xi)$ into a function of two variables. Nonetheless, an inversion formula is available

$$H(\xi)=\frac{1}{2\pi}\int_{-\infty}^{+\infty}\int_{-\infty}^{+\infty}\mathcal{G}(\omega,\tau)W_{\omega,\tau}(\xi)d\omega d\tau \tag{3}$$

allowing to recover the original function from its coefficients. The theory of Gabor and more general time-frequency decompositions is well-known and many mathematical properties have been proved (see [6] and references therein). The main result that we will exploit in this work is that $|\mathcal{G}(\omega,\tau)|^2$, sometimes called *spectrogram*, represents the time-frequency decomposition of the energy of $H(\xi)$. Also, we will use the fact that the reconstruction formula (3) can be combined with a time-frequency localization process in order to split $H(\xi)$ into separate components. More precisely,

$$H(\xi)=\sum_{k=1}^{K}H_k(\xi)\,,\quad H_k(\xi)=\frac{1}{2\pi}\iint_{\Omega_k}\mathcal{G}(\omega,\tau)W_{\omega,\tau}(\xi)d\omega d\tau\,,\quad \bigcup_{k=1}^{K}\Omega_k=\Re^2\,. \tag{4}$$

In other words, the entire time-frequency plane (ω,τ) can separated into disjoint subsets Ω_k. Integration over each of those regions leads to a partial reconstruction $H_k(\xi)$. The superposition of all partial components leads exactly to the original function $H(\xi)$.

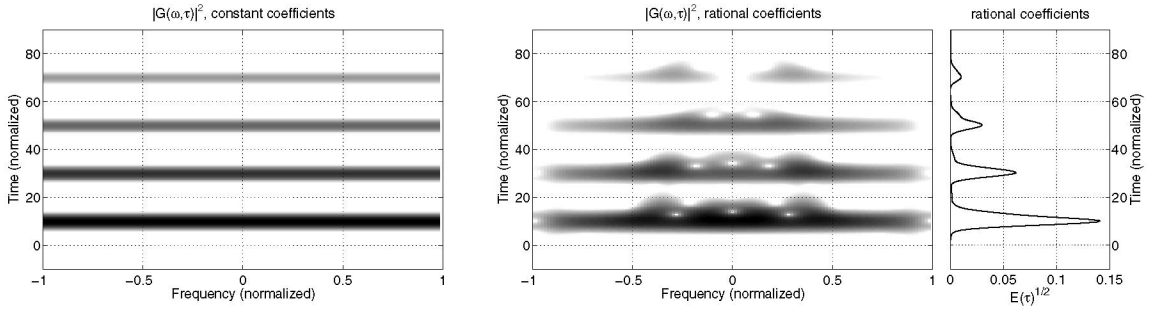

Figure 2: Time-frequency energy distribution $|\mathcal{G}(\omega,\tau)|^2$ for the synthetic examples of Sec.2. Constant coefficients (left) and rational coefficients (middle). Right panel is the RMS ω-average of the coefficients in middle panel.

The reason for the introduction of the Gabor transform for present application is illustrated by two simple examples. First, we consider a synthetic response of the form

$$S(s) = \sum_{k=1}^{K} A_k e^{-sT_k}, \quad \text{with} \quad K = 4, \quad A_k = (0.5)^{k-1}, \quad T_k = 10 + 20k. \tag{5}$$

over a normalized unitary frequency band. This example represents the transmission response of a mismatched ideal transmission line with resistive terminations. The (normalized) time-frequency energy distribution $|\mathcal{G}(\omega,\tau)|^2$ is depicted in the left panel of Fig. 2. The delays are well resolved by the transform, which also shows that the frequency behavior of the single-delay atoms is constant, as expected. Conversely, the amplitude of the single-delay atoms is decreasing for increasing delay, coherently with (5).

The second example is similar, but we replace the constant coefficients in (5) with rational frequency-dependent coefficients $A_k(s)$ constructed as fourth order rational functions with randomly-selected poles and residues. The corresponding energy distribution $|\mathcal{G}(\omega,\tau)|^2$ is depicted in the middle panel of Fig. 2. It should be noted that although the coefficients are now frequency-dependent, the localization of the time delays is still excellent. This fact will enable the separation of the single-delay atoms, as described in Sec. 3.

A final remark on discretization issues. The transform in (2)-(3) is continuous and defined on an infinite domain. Therefore, some discretization and truncation must be performed in order to apply this tool to finite-bandwidth sampled responses. The natural choice is to constrain $\omega = n\omega_0$ and $\tau = m\tau_0$. This discretization leads to technical complications, since a pair of dual window functions $\{W(\xi), \widetilde{W}(\xi)\}$ must be used for the transform and its inverse, respectively. The actual shape of the dual window depends on the resolution of the time-frequency discretization lattice. The theory of *frames* provides all mathematical details [6]. Of course, all the results in this work have been produced with the discrete Gabor transform, although the theoretical formulation adopts the continuous transform for simplicity.

3 Separation and approximation of single-delay atoms

We now describe how the single-delay atoms can be separated based on the Gabor coefficients. We average the time-frequency energy distribution via

$$\mathcal{E}(\tau) = \frac{1}{2\pi} \int_{-\infty}^{\infty} |\mathcal{G}(\omega,\tau)|^2 d\omega \,. \tag{6}$$

This quantity presents well-pronounced maxima corresponding to the delays $\widetilde{T}_k$, as clearly seen from the right panel of Fig. 2. The minima between each pair of maxima, which we denote as τ_k, can be used to separate the single-delay atoms. Therefore, we define

$$\Omega_k = \{(\omega,\tau) : \ \tau \in (\tau_k, \tau_{k+1}), \ \forall\omega\} \tag{7}$$

as horizontal strips in the (ω,τ) plane. The single-delay atoms $H_k(\xi)$ are then obtained by applying Eq. (4).

Each local maximum $\widetilde{T}_k$ of $\mathcal{E}(\tau)$ provides a good estimate for the delay associated to the corresponding single-delay atom. However, we refine this estimate by applying a procedure similar to [5]. Assuming that the true delay is $\widehat{T}_k$, a tentative delay-free atom is defined as $H_k(\xi)e^{+j\xi\widehat{T}_k}$. Then, VF is applied to compute its rational approximation, and the VF approximation error $\varepsilon_k(\widehat{T}_k)$ is computed. The optimum delay T_k is determined by minimizing the error $\varepsilon_k(\widehat{T}_k)$ over a suitable (small) interval centered at $\widetilde{T}_k$.

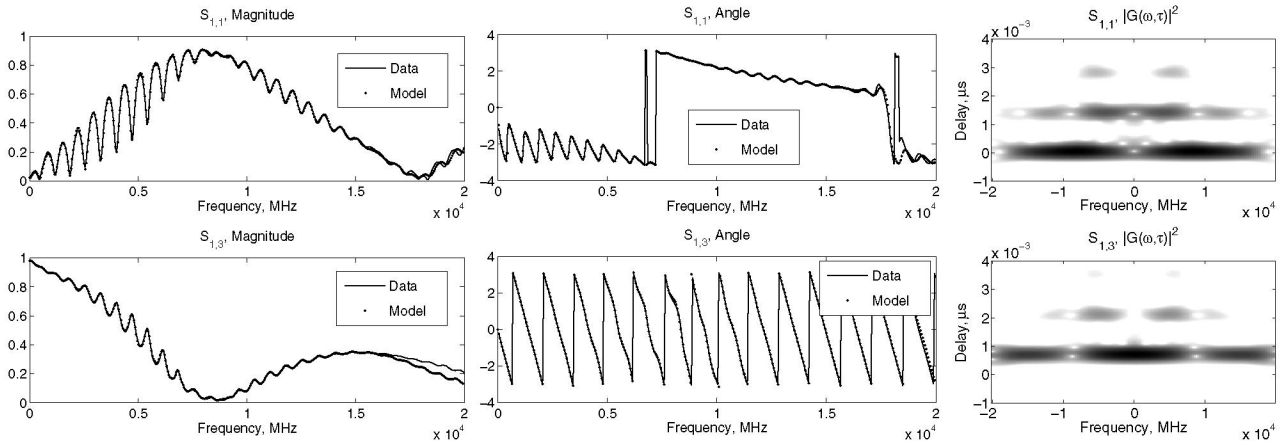

Figure 3: Model validation for $S_{1,1}$ (top row) and $S_{1,3}$ (bottom row). Right panels depict the Gabor transform energies.

The above procedure results in a delayed rational approximation of each single-delay atom, as formulated in Eq. (1). The algorithm is fully automatic and is applicable to "black-box" frequency responses, such as direct measurements. The only approximation error which is involved in this global macromodeling scheme is due to the rational fit, since the inversion of the Gabor transform is exact up to machine precision. In summary, the Gabor transform is used as a tool for the localization of the single-delay atoms, which are then approximated via standard techinques. This last operation is possible because only one dominant delay is attributed to each atom.

4 Numerical results

We apply the proposed macromodeling technique to a set of measured scattering responses of a PCB interconnect link (courtesy of C. Schuster, IBM). We present results for the return loss and for the insertion loss. Since we are dealing with measured data, we apply a thresholding procedure to the Gabor transform and retain only the coefficients such that $|\mathcal{G}(\omega,\tau)|^2 > \epsilon$, in order to perform data denoising. This induces a reconstruction RMS relative error δ in the inversion of the Gabor transform, which amounts in present case to $\delta = 0.009$ for $S_{1,1}$ and to $\delta = 0.007$ for $S_{1,3}$. The right panels in Fig. 3 depict the thresholded Gabor coefficients, showing the presence of three significant distinct delay terms for each of the two responses. The automatic identification of these delays led to $T_k = \{0,\ 1.31,\ 2.86\}$ ns for $S_{1,1}$ and to $T_k = \{0.67,\ 2.01,\ 3.38\}$ ns for $S_{1,3}$. A VF-based rational fit resulted in $\{6,\ 8,\ 4\}$ poles and $\{8,\ 10,\ 4\}$ poles for $S_{1,1}$ and $S_{1,3}$ single-delay atoms, respectively. A comparison between model and raw data is shown in Fig. 3. The accuracy is excellent. Only a small deviation in the insertion loss magnitude is visible, due to the fact that we constrained the model response to be vanishing for large frequency. Based on these preliminary results, the proposed technique seems to be very promising for the generation of low-complexity models for long interconnect links characterized by significant propagation delays.

References

[1] B. Gustavsen, A. Semlyen, "Rational approximation of frequency responses by vector fitting", *IEEE Trans. Power Delivery*, Vol. 14, July 1999, pp. 1052–1061.

[2] S. Grivet-Talocia, H. M. Huang, A. E. Ruehli, F. Canavero, I. M. Elfadel, "Transient Analysis of Lossy Transmission Lines: an Effective Approach Based on the Method of Characteristics" , *IEEE T-ADVP*, Vol. 27, N. 1, 2004, pp. 45–56.

[3] R. Mandrekar, M. Swaminathan, "Causality enforcement in transient simulation of passive networks through delay extraction", 9th IEEE Workshop on Signal Propagation on Interconnects, 2005, pp. 25–28.

[4] Bing Zhong, Tao Hu, D. Fu, S.L. Dvorak, J.L. Prince, "A study of a hybrid phase-pole macromodel for transient simulation of complex interconnects structures", *IEEE T-CAD*, Vol. 24, N. 8, Aug. 2005, pp. 1250–1261.

[5] B. Gustavsen, "Time delay identification for transmission line modeling", 8th IEEE Workshop on Signal Propagation on Interconnects, 2004, pp. 103–106.

[6] I. Daubechies, *Ten Lectures on Wavelets*, Philadelpia: SIAM, 1992.